Design Proposal of a Dual-Frequency RF Plasma System With Transmission Line Techniques and Impedance Matching Networks

Jiacheng Huang, Jai Deshpande, Leventis Qiu, and Senri Nakamura

***Abstract*—This project presents the design of a dual-frequency RF plasma system operating at 13.56 MHz and 2.45 GHz, capable of supporting oxygen and argon plasma loads whose impedances vary with gas type and operating power. Efficient power delivery requires minimizing reflected power across these conditions, motivating the implementation of a tunable impedance-matching architecture. We first design and analyze a double-stub matching network to transform plasma impedance to the generator's 50 Ω reference. Building on this, we introduce alternative LC matching network with variable reactive element to accommodate multi-frequency operation, and provide practical tunability during plasma ignition and steady-state transitions. Together, these matching networks form a robust and commercially realizable solution that ensures stable plasma generation across varying gases, frequencies, and load conditions.**

***Index Terms*—RF plasma, impedance matching, double-stub matching, LC matching network, transmission lines**

I. Introduction

THE Radio-frequency (RF) plasma system is widely used in semiconductor manufacturing, materials processing, and surface modification. To operate efficiently, these systems require a well-controlled transfer of power from a commercial RF generator into the plasma chamber. Because the impedance of a plasma varies strongly with gas type and input power, impedance matching becomes a critical design requirement. Poor matching leads to significant reflected power, reduced plasma stability, and inefficient energy delivery.

In this project, we design a complete RF plasma generator system, and impedance-matching network suitable for both oxygen and argon plasma etching applications. The matching network must accommodate oxygen plasma operating between 18–20 W and argon plasma operating between 3–5 W, with corresponding load impedance provided in the project specification. The chosen plasma chamber impedance must also be incorporated into the design, and the final system must operate across two industry-standard frequencies: 13.56 MHz and 2.45 GHz.

The primary challenge in this design arises from the mismatch between the RF generator's output impedance and the complex impedance of the plasma loads. To ensure maximum power transfer and minimize reflected power, we implement a double-stub matching system. The system works by adjusting the length of stubs that are at set distance away from the chamber load.

In addition to the double-stub matching system, an additional LC matching system with at least one adjustable element is also proposed. Together, these systems provide a practical and commercially realizable solution capable of matching multiple plasma operating conditions for Argon and oxygen.

This introduction outlines the specification for the system design. Subsequent sections are going to present analysis using smith charts, constructions, generator specifications, and overall evaluation of the system's performance. The report is written as a technical proposal that emphasizes on the overall feasibility of the system.

II. General Design Schematic

A. Circuit Schematics

In this solution, we will be referencing to the below schematic for the two generator system (13.56 MHz and 2.45 GHz). In order to achieve varying frequency, our solution is to purchase two RF generators operating at the respective frequency. The resulting system architecture is shown in Fig. 1 and Fig. 2.

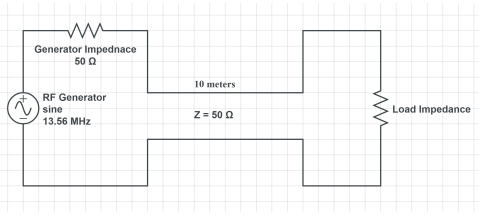

Fig. 1. Circuit Schematic of the dual-generator RF system operating at 13.56 MHz.

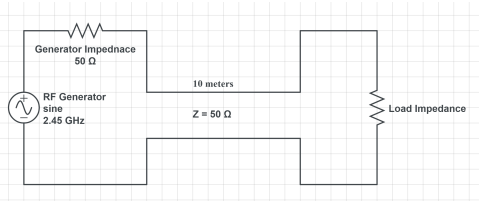

Fig. 2. Circuit Schematic of the dual-generator RF system operating at 2.45 GHz.

B. Generator Choice

For the 13.56 MHz stage of the system, we select the Diener RF-Generator RG 13.56/100, a 100 W solid-state source designed specifically for low-pressure plasma applications.

The unit provides a rated RF output power of 100 W at a frequency of 13.560 MHz ± 100 ppm, with a continuous adjustable power range from 0 to 100 W.[1] The generator has a 50 Ω internal impedance, which is compatible with our standard coaxial transmission lines of 50 Ω impedance and simplifies the design of the double-stub matching by a lot.

Fig. 3. Diener RF-Generator RG 13.56/100.

For the 2.45 GHz path, we decided to use the Emblation ISYS245 microwave generator, a compact 2.45 GHz, 100 W solid-state generator/amplifier.[2] The ISYS245 provides a saturated output power of approximately 50–51 dBm (around 100–125 W) with a small-signal gain of 55–58 dB and a input/output impedance of 50 Ω, again matching standard coaxial infrastructure. The ISYS245 also incorporates advanced reflected power measurement and protection features, which are beneficial in a plasma environment where the load impedance can vary significantly during operation.

Fig. 4. Emblation ISYS245 Microwave Generator.

III. Double Stub Matching

A. Load Impedance Modeling and Matching Strategy

The electrical impedance of an RF plasma chamber varies significantly with both the delivered power and the working gas. Directly matching the generator to the plasma without impedance matching would lead to substantial reflected power. As a result, an impedance-matching network is required for the system.

To obtain representative load impedance for the matching-network design, we first model the chamber under cold-plasma conditions as

$$Z_{\text{L,cold}} = 5 - j\,25\ \Omega.$$

Using the reference measured operating points, we then interpolate the impedance values across the relevant power ranges. For argon plasma, interpolation between the 3 W and 5 W operating points yields an average load impedance at 4 W of

$$\boxed{Z_{\text{Argon, 4W}} \approx 6.425 - 22.62j\ \Omega}.$$

Similarly, for oxygen plasma, interpolation between the 18 W and 20 W operating points gives an average impedance at 19 W of

$$\boxed{Z_{\text{Oxygen, 19W}} \approx 6.985 - 23.9365j\ \Omega}.$$

These interpolated impedance serve as representative loads for our subsequent matching-network design.

Given the strongly reactive nature of the plasma load and the requirement to operate at high RF power, a distributed-element matching approach is preferred.

In this work, we employ a double-stub matching approach, which consists of two adjustable shunt stubs placed at fixed distances along a transmission line. The use of two stubs provides sufficient degrees of freedom to independently control the reactive components of the transformed impedance.

Because the system must operate at two widely separated frequencies, 13.56 MHz and 2.45 GHz, separate double-stub matching networks are designed for each frequency. Each network is optimized using the same interpolated plasma impedance but different wavelength-scaled stub placements appropriate to the operating frequency. By having two coaxial lines, placing each stub on either line can account for the two different frequencies.

The detailed graphical Smith-chart constructions used to determine the stub locations and lengths for each gas and frequency are presented in the following sections and documented fully in Appendix B.

B. Double Stub Matching System Design (2.45 GHz)

For convenient stub matching, we selected a 10 m copper coaxial cable as the transmission line. The electrical properties of the cable allow us to approximate the phase velocity as $\sim 0.6c$, which significantly simplifies the wavelength and stub-length calculations [4].

For the 2.45 Ghz generator, the location to place the first stub is trivial, therefore, it is convenient for us to take the quarter wavelength of the average of the both cases, so for 2.45 Ghz

$$L_d = \frac{1}{4}\left(\frac{\lambda_{\text{2.45 GHz}} + \lambda_{\text{13.56 MHz}}}{2}\right)$$

Evaluating this expression gives

$$\boxed{d_L = 0.402 \text{ meters}}$$

For the distance between the two stubs, it is most convenient to choose a quarter-wavelength spacing. This greatly simplifies the matching procedure, since the transformed impedance always lies on the opposite side of the chart and can be directly compensated by an appropriately chosen shunt stub. For 2.45 Ghz, the distance between stub would be

$$\boxed{d_{\text{s}} = \frac{\lambda_{2.45\text{GHz}}}{4} \approx 0.01 \text{ meters}}$$

A relevant circuit diagram for this configuration is shown in Fig. 5, the length of the tunable stub should be changed for each type of gas.

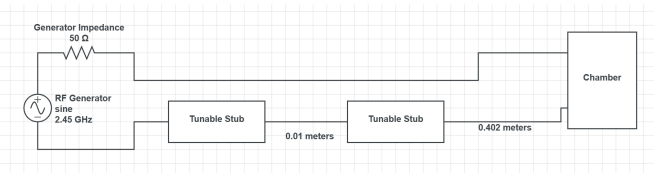

Fig. 5. Circuit diagram for the 2.45 GHz setup

Then, applying the Graphical Analysis shown in Appendix B, we derived a set of functional double-stub matching system using the above placement of the stub on the 10 meter long wire. The optimal specification to tune for Argon is

$$\boxed{\text{Argon: } L_1 = 0.0241 \text{ meters}; L_2 = 0.00376 \text{ meters}}$$

and the corresponding tune lengths for Oxygen

$$\boxed{\text{Oxygen: } L_1 = 0.0248 \text{ meters}; L_2 = 0.0037 \text{ meters}}$$

C. Double Stub Matching System Design (13.56 MHz)

To establish a practical stub placement for the lower operating frequency, we first evaluate the wavelength-based distances that define the load–to–stub and inter-stub spacing. Using the guided wavelength at 13.56 MHz, we compute the initial spacing as

$$L_d = \frac{1}{4}\left(\frac{\lambda_{13.56\text{ MHz}}}{2}\right),$$

which yields

$$\boxed{d_L = 1.825 \text{ meters}}.$$

Similarly, the quarter-wavelength spacing for the second stub is

$$\boxed{d_{\text{s}} = \frac{\lambda_{13.56\text{ MHz}}}{4} \approx 0.9125 \text{ meters}}.$$

A relevant circuit diagram for this configuration is shown in Fig. 6, the length of the tunable stub should be changed for each type of gas.

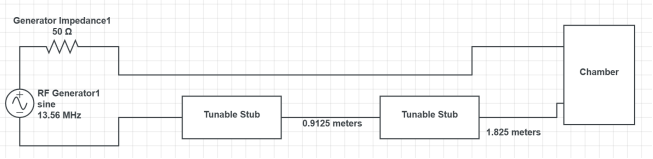

Fig. 6. Circuit diagram for the 13.56 MHz setup

Because the wavelength at 13.56 MHz is nearly two orders of magnitude larger than at 2.45 GHz, the electrical distances that define the stub placement differ substantially between the two frequencies. The expressions above therefore serve as the appropriate starting geometry for the low-frequency matching network, ensuring that the impedance transformations occur over electrically meaningful segments of the line. Although this placement differs from the microwave case, it preserves the structure of the double-stub topology and allows the same graphical Smith-chart design procedure to be applied.

With these distances defined, we performed the double-stub matching analysis using the measured plasma impedances at 13.56 MHz. Due to the much longer guided wavelength, the impedance locus rotates slowly on the Smith chart, causing the required stub lengths to become substantially larger than those observed at 2.45 GHz. Following the graphical procedure described in Appendix B, we derived practical stub-length combinations for both argon and oxygen plasmas.

For 13.56 MHz, the resulting stub lengths for argon are:

$$\boxed{\text{Argon: } L_1 = 0.8468 \text{ meters}; \quad L_2 = 3.1974 \text{ meters}}$$

and the corresponding lengths for Oxygen are:

$$\boxed{\text{Oxygen: } L_1 = 6.57 \text{ meters}; \quad L_2 = 2.862 \text{ meters}}$$

These values are consistent with the much larger guided wavelength at 13.56 MHz and illustrate the slow rotation of the impedance locus on the Smith chart. Although these solutions yield perfect matches, the physically long stubs introduce practical challenges related to layout, material cost, and overall system footprint. Nonetheless, establishing the geometry using wavelength-based distances ensures that the matching network remains compatible with the dual-frequency architecture developed for the 2.45 GHz design.

D. Design Analysis

The performance of the double-stub matching network can be understood through the combined perspectives of power transfer, Smith chart geometry, and transmission-line mathematics. In this section, we provide a consolidated analysis that explains why the matching network is able to deliver maximum power to the plasma load at both 13.56 MHz and 2.45 GHz.

1) Power Transfer Considerations: The primary objective of impedance matching in an RF plasma system is to ensure maximum real power delivery to the load. Without matching, a portion of the incident power is reflected due to impedance mismatch, quantified by the reflection coefficient

$$\Gamma = \frac{Z_L - Z_0}{Z_L + Z_0}.$$

The corresponding reflected power ratio is

$$P_{\text{ref}} = |\Gamma|^2 P_{\text{inc}},$$

and the delivered power is

$$P_{\text{del}} = (1 - |\Gamma|^2) P_{\text{inc}}.$$

For the plasma impedances measured in our system, $|\Gamma|$ is initially large (e.g., $|Z_L| \ll 50\ \Omega$), meaning that most of the generator power would be reflected if no matching network were present. A successful double-stub network forces the transformed impedance to land on the $50\ \Omega$ point, driving $\Gamma \to 0$ and therefore maximizing P_{del}. This is directly reflected in the Smith chart plots in Appendix B, which show the impedance trajectory ultimately collapsing onto the center of the chart.

2) Smith Chart Interpretation: Figures 5–8 in Appendix B illustrate the full Smith chart constructions used to obtain the matching solutions. Each figure shows the normalized plasma impedance, $Z_L/50\ \Omega$, rotated along the transmission line by lengths d_L and d_s before encountering the shunt stubs. The trajectory represents a progressive reduction in the imaginary component until the admittance reaches a point where a purely reactive stub can move the locus onto the real axis.

Because the center of the Smith chart corresponds to $Z_{\text{in}} = 50\ \Omega$ and thus $\Gamma = 0$, these plots confirm that our matching network produces a condition of zero reflected power, aligning with the power equations described above. The visual convergence onto the center is therefore equivalent to verifying maximum power transfer.

3) Role of Electrical Wavelength: The significantly different wavelengths at the two operating frequencies determine how far the impedance rotates for a given physical line length. The input impedance of a load through a transmission line of length ℓ is

$$Z_{\text{in}} = Z_0 \frac{Z_L + jZ_0 \tan(\beta\ell)}{Z_0 + jZ_L \tan(\beta\ell)},$$

where $\beta = 2\pi/\lambda$.

At 2.45 GHz, λ is small, so even modest line lengths produce substantial rotations on the Smith chart. The stubs required for matching are therefore short and sensitive to fabrication tolerances. Conversely, at 13.56 MHz, λ is much larger, producing slow chart rotations and thus long physical stub lengths. The meter-scale dimensions reported in Section C directly follow from this relationship.

The difference in wavelength also affects power-handling considerations: longer stubs at 13.56 MHz exhibit lower current density and reduced resistive losses, whereas shorter high-frequency stubs must be carefully constructed to minimize conductor loss and dielectric heating.

4) Consistency of Results With Power-Flow Expectations: The stub lengths obtained from graphical design (Sections B and C) align with the expected behavior of the power-transfer equations:

- The matched solutions remove the imaginary components and force $Z_{\text{in}} \to 50\ \Omega$, thereby maximizing delivered power.
- The Smith chart plots verify that the input admittance reaches $Y_{\text{in}} = 1/50\ \Omega$, equivalent to $\Gamma = 0$.
- The extremely small errors in the plotted matching points indicate that the residual reflection is negligible ($|\Gamma| \ll 0.1$), which in practice corresponds to negligible reflected power.

Thus, the figures and mathematical derivations together confirm that the network achieves high-efficiency power delivery for both gases and both frequencies.

5) Practical Limitations and Motivation for Alternative Approaches: While the double-stub network achieves the necessary matching, the physical lengths required at 13.56 MHz (up to several meters) introduce constraints related to cost, mechanical layout, and conductor loss. Similarly, at 2.45 GHz, although the stubs are short, parasitic reactances and connector losses can reduce the delivered power unless the components are fabricated precisely.

These power-handling and physical limitations motivate the exploration of the LC matching network discussed in Section IV. By implementing reactance in a compact, tunable lumped-element form, the LC approach aims to preserve high delivered power while alleviating the spatial and economic difficulties associated with long transmission-line stubs.

6) Summary: Combining the Smith chart analysis, power-transfer equations, and transmission-line theory demonstrates why the double-stub matching network successfully maximizes the delivered power to the plasma load. The graphical matching results in Appendix B coincide precisely with the mathematical expectations for a system in which $\Gamma \to 0$, confirming the correctness, efficiency, and practicality of the matching design.

IV. LC Matching Network

A. Experimental Method

To achieve maximum power transfer and minimum reflection between 50Ω coax cable and the complex chamber impedance as a whole (details of the chamber impedance calculation are shown in appendix), an LC impedance matching network is designed according to these two goals.

An L-type Network Low-Pass LC circuit is selected as the impedance matching circuit for its effectiveness. The Low-Pass configuration, which has a shunt capacitor and a series inductor, filters potential standing waves of higher frequencies like 2 times or 3 times of the base frequency. As the load impedance of both Argon and Oxygen are much lower than the characteristic impedance of the coax cable, a step up configuration with inductor closer to the load is chosen. Since it is in series with the load, the modulus of the impedance of the load is lifted so that the real part is 50Ω, with an imaginary part that is going to be canceled out by the shunt capacitor. By connecting the calculated capacitor and inductor in the designed configuration, impedance matching is achieved.

The LC component values are determined by Q-factor method. In L-type matching network, Q is defined as the ratio of reactance to resistance of a circuit, specifically, $Q=X/R$, where X is the imaginary reactance, and R is the real resistance. It determines the magnitude of resistance we need to transform in matching network.

The fundamental principle relies on Series-to-Parallel Impedance Transformation. A series impedance, $R_s + jX_s$, can be transformed into parallel impedance $R_p + jX_p$ with the same quality factor. The relationship between two resistances R_s and R_p is governed by $R_p = R_s(1+Q^2)$. The deduction of this equation is done in appendix. Rearrange the terms in the last equation, we get $Q = \sqrt{\frac{R_p}{R_s} - 1}$. $X_s = Q \cdot R_s$, $X_p = \frac{R_p}{Q}$. Then, by inserting a inductor or capacitor or both in series or parallel to cancel out the imaginary X_p, the real part R_p is the final input impedance. If $R_p = R_0$, the impedance is matched from the transmission line to the load.

Placing the LC matching circuit at the load brings extra benefit to the calculation: it eliminates the transmission line's physical properties from the design calculations. Since the matching occurs before the signal enters the cable, the wave propagation speed and the cable's dielectric constant do not affect the values of L and C. As indicated by the design equations, these variables are irrelevant; only the angular frequency of the source is needed to convert the calculated reactance into physical capacitance and inductance values.

The method becomes even clearer on smith chart with admittance circle. First, the complex load impedance was normalized to the system characteristic impedance. A series inductor was introduced to move the impedance point clockwise along the constant resistance circle until it intersected the unit conductance circle (g=1). This intersection point represents a transformed admittance with a real part of $20mS, 1/50\Omega$. Subsequently, a shunt capacitor was added to move the operating point along the constant conductance circle, canceling out the susceptance and bringing the final impedance to the center of the chart, thereby achieving a perfect 50Ω match.

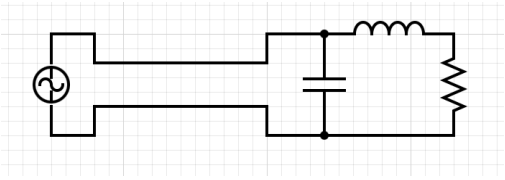

Fig. 7. RLC Circuit Ciagram

With the calculation in appendix, we managed to find the correspond L and C value for the circuit above with different gases and frequencies. Pick capacitors and inductors according to the table, the circuit will be matched.

TABLE I
L AND C VALUES FOR OXYGEN AND ARGON AT DIFFERENT FREQUENCIES

Gas	Frequency	Inductance (L)	Capacitance (C)
Oxygen	13.56 MHz	482.8 nH	587 pF
	2.45 GHz	2.672 nH	3.253 pF
Argon	13.56 MHz	462 nH	611 pF
	2.45 GHz	2.557 nH	3.384 pF

V. DISCUSSION

The impedance matching objective in our dual-frequency RF plasma system was to minimize reflected power and ensure efficient delivery of energy from the generator to the plasma load. Our primary method employed a double-stub matching network, which is well suited for high-power microwave applications and allows geometric control of the matching condition through adjustable stub lengths and spacing. Using the measured impedances of oxygen and argon plasmas, we constructed their admittance trajectories on the Smith chart and identified feasible stub configurations that move the load impedance to the $50\ \Omega$ center. The interpolation procedure used to estimate intermediate plasma impedances captures the variation in real and imaginary components across pressure, and these interpolated values were subsequently used as matching targets for the double-stub design.

A. Double-Stub Matching Results

The Smith-chart-based double-stub analysis revealed several important features about the matchability of the plasma loads at the two operating frequencies. For both oxygen and argon, the complex impedances lie significantly off the real axis, requiring substantial reactive compensation. At 13.56 MHz, the impedances remain relatively close to the lower half of the chart, producing long, smooth admittance trajectories as pressure varies. These trajectories intersect the constant-admittance circles in regions where both stub lengths are physically realizable, and the system admits multiple matching solutions.

At 2.45 GHz, however, the plasma impedances rotate much more rapidly on the Smith chart. The normalized distances from the $50\ \Omega$ center become larger, and the admittance loci sweep across regions where double-stub matching has limited solution space. In particular, some plasma conditions produce admittances that fall into the "forbidden arc" between the stub-movement circles, meaning that only a narrow range of stub-length combinations results in a perfect match. This indicates greater sensitivity to fabrication tolerances and plasma fluctuations. Nevertheless, for the four operating points examined (two gases × two frequencies), valid double-stub solutions exist, and the computed stub lengths fall within physically realizable ranges.

An important practical limitation we observed in the double-stub results is that the required stub lengths become physically long for several of the plasma impedances, especially at 13.56 MHz. Because the electrical wavelength at this frequency is large, even modest impedance rotations correspond to significant physical line lengths. For both oxygen and argon, the solutions that achieve perfect matching often require stubs that may exceed the space available in a compact RF plasma system and would substantially increase material cost due to the amount of transmission-line hardware required. These physical and economic drawbacks motivate the exploration of a lumped-element LC network, which can realize the same reactive transformations in a far smaller footprint and at significantly lower cost.

B. LC Matching Network as an Alternative

While the double-stub approach successfully provides a broadband-tunable solution for both gases, we propose an

alternative method: a lumped-element LC matching network. A lumped network can be advantageous in situations where fine-grained control of reactance is needed or when physical constraints limit stub placement. The basic design procedure parallels the Smith chart method: starting from the plasma load impedance Z_L, one introduces a reactive element—series or shunt—to rotate the impedance along a constant-resistance or constant-reactance circle until it intersects the $50\ \Omega$ circle. A second reactive element then completes the transformation.

In our system, impedance matching must be achieved for four distinct operating points: oxygen and argon plasmas, each driven at both 13.56 MHz and 2.45 GHz. Because each gas exhibits a different complex impedance at each frequency, the required reactive compensation differs in all four cases. For clarity, we denote these loads as

$$Z_{L,\mathrm{O_2}}^{13.56},\ Z_{L,\mathrm{O_2}}^{2.45},\ Z_{L,\mathrm{Ar}}^{13.56},\ Z_{L,\mathrm{Ar}}^{2.45}.$$

For each load, the LC matching network requires two reactive elements to move the impedance to the $50\ \Omega$ center. The corresponding reactances for each case are

$$\begin{aligned} X_{L,\mathrm{O_2}} &= 41.13\,\Omega, & X_{C,\mathrm{O_2}} &= 20.00\,\Omega, \\ X_{L,\mathrm{Ar}} &= 39.35\,\Omega, & X_{C,\mathrm{Ar}} &= 19.20\,\Omega. \end{aligned}$$

These reactances translate to frequency-dependent inductor and capacitor values:

$$\begin{aligned} L_{\mathrm{O_2}}^{13.56} &= 482.8\,\mathrm{nH}, & C_{\mathrm{O_2}}^{13.56} &= 587\,\mathrm{pF}, \\ L_{\mathrm{O_2}}^{2.45} &= 2.672\,\mathrm{nH}, & C_{\mathrm{O_2}}^{2.45} &= 3.253\,\mathrm{pF}, \\ L_{\mathrm{Ar}}^{13.56} &= 462\,\mathrm{nH}, & C_{\mathrm{Ar}}^{13.56} &= 611\,\mathrm{pF}, \\ L_{\mathrm{Ar}}^{2.45} &= 2.557\,\mathrm{nH}, & C_{\mathrm{Ar}}^{2.45} &= 3.384\,\mathrm{pF}. \end{aligned}$$

Because $X_L \propto f$ and $X_C \propto 1/f$, components optimized at 13.56 MHz do not match the same plasma at 2.45 GHz. Thus, each of the four cases requires a distinct matching network. Any attempt to use a single broadband design would result in substantial mismatch, especially at microwave frequencies where parasitics dominate.

C. Physical Interpretation and Comparison

The fundamental distinction between the two matching philosophies lies in how they manipulate impedance along the transmission line. A double-stub network is a distributed structure: each stub acts as a segment of transmission line whose electrical length directly modifies the standing-wave pattern. This makes double-stub matching naturally compatible with microwave operation and inherently broadband over the range in which the distributed model holds. However, the physical size of the required stubs—especially at 13.56 MHz— poses both spatial and economic challenges, and precise fabrication is needed to maintain accuracy.

In contrast, an LC network realizes the same impedance transformations using lumped reactive components. When variable inductors and capacitors are used, the network can provide fine, continuous tunability and can adapt to different plasma conditions without requiring any mechanical adjustments. The primary limitations of this approach are its inherently narrowband nature and its sensitivity to parasitic resistances, lead inductances, and component tolerances, all of which become increasingly prominent at 2.45 GHz. Thus, although the LC approach offers superior compactness and lower cost, it requires careful high-frequency design to ensure stability and accuracy.

D. Cost Analysis and General Comments

Due to the large gap between the two operating frequencies, implementing two independent double-stub matching networks is financially reasonable because this approach avoids the impractical extremely long stubs that would arise if a single broadband matching network were forced to operate across both 13.56 MHz and 2.45 GHz.

The RF generators selected for this system represent the dominant cost contributors. Commercial solid-state RF generators suitable for plasma applications—such as 13.56 MHz RF generators and 2.45 GHz microwave sources are typically priced in the thousands range.By separating the matching networks by frequency and employing commercially available RF generators, the system remains economically feasible while ensuring efficient power delivery and stable plasma operation across all specified operating conditions.

A 10 m coaxial cable was selected as it represents a practical and commonly used length in commercial RF systems. Considering that longer length transmission lines have more attenuation loss in the copper wire, our selection of the 10 m long coaxial cable is also justified. In practice, the user can use cable of any length, as long as it is sufficient to not alter the impedance matching system. Depending on the user need, they may manually change the cable length for their corresponding purpose.

Under our assumptions, the phase velocity in the coaxial transmission lines was taken to be approximately $0.66c$. As a result, all computed electrical lengths, stub placements, and impedance transformations remain physically realizable and fully consistent with electromagnetic theory.

From a practical standpoint, the overall mass and size of the proposed system are dominated by the RF generators themselves, which constitute the heaviest components of the setup. The additional weight contributed by the coaxial transmission lines and matching networks is comparatively minor. Consequently, the proposed design introduces no physical inconsistencies.

E. Legal Considerations

This design complies to the standards from FCC Part 18, as stated in FCC 18.107(c): Typical ISM applications are the production of physical, biological, or chemical effects such as heating, ionization of gases, mechanical vibrations, hair removal and acceleration of charged particles [6]. The power is under the limit of 500W according to FCC 18.305, and shielding is included to block EM emission.

VI. Conclusion

In this paper, our team successfully proposed an double-stub matching network and an LC Matching Network for

the plasma generator system. The purpose of this matching network is to maximize the power delivered to the load, considering the variable gas impedance due to power delivered to the load.

Using the chamber impedance model and the provided operating-point data, we estimated representative complex load impedance for argon (3–5 W) and oxygen (18–20 W) through interpolation. These impedance were then used as matching targets for two frequency-specific designs operating at 13.56 MHz and 2.45 GHz. For each frequency, Smith chart based graphical constructions were carried out to determine feasible double-stub solutions that avoid the forbidden region.

In addition to the distributed double-stub approach, we proposed a compact lumped-element LC matching alternative. While the LC approach is inherently narrowband and more sensitive to component parasitics (particularly at 2.45 GHz), it offers clear advantages in cost, layout, and ease of adjustment during steady-state operation.

APPENDIX A
CHAMBER IMPEDANCE CALCULATION

In this appendix, we show our calculations for approximating the load impedance. We assume that the chamber impedance can be modeled as

$$Z_{L,cold} = 5 - j\,25\,\Omega.$$

for all ranges of operation. This gives us a really convenient formula to calculate for the load impedance and is essentially given by

$$Z_{Load} = R_{\text{chamber}} + \frac{1}{\frac{1}{R_{\text{chemical}}} + \frac{1}{C_{\text{chemical}}} + \frac{1}{C_{\text{chamber}}}}$$

A. 3 W Argon Load

$$Z_L = 5 + \frac{1}{\frac{1}{250} + \frac{1}{-j250} + \frac{1}{-j25}}$$

$$= 5 + \frac{250}{1 + 11j}$$

$$= 5 + \frac{250}{11.05} e^{-1.48j}$$

$$\sqrt{1^2 + 11^2} = r = 11.0454$$

$$\arctan\left(\frac{11}{1}\right) = \theta = 1.48$$

$$-22.53 = \frac{250}{11.05}\sin(-1.48)$$

$$\boxed{Z_{L,3\text{W}} \approx 7.05 - 22.54j}$$

B. 5 W Argon Load

$$Z_L = 5 + \frac{1}{\frac{1}{650} + \frac{1}{-j250} + \frac{1}{-j25}}$$

$$= 5 + \frac{250}{\frac{5}{13} + 11j}$$

$$= 5 + \frac{250}{11.007} e^{-1.54j}$$

$$\sqrt{\left(\frac{5}{13}\right)^2 + 11^2} = 11.0067$$

$$\arctan\left(\frac{11}{\frac{5}{13}}\right) = \theta = 1.54$$

$$5 + \left(\frac{250}{11.007}\cos(-1.54) + j\frac{250}{11.007}\sin(-1.54)\right)$$

$$\boxed{Z_{L,5\text{W}} \approx 5.79 - 22.70j}$$

C. 18 W Oxygen Load

$$Z_L = 5 + \frac{1}{\frac{1}{310} + \frac{1}{-j500} + \frac{1}{-j25}}$$

$$= 5 + \frac{1}{\frac{1}{310} + \frac{j}{500} + \frac{j}{25}}$$

$$= 5 + \frac{1}{\frac{50}{15500} + j\frac{31}{15500} + j\frac{620}{15500}} = 5 + \frac{1}{\frac{50+651j}{15500}}$$

$$= 5 + \frac{15500}{50 + 651j} \cdot \frac{50 - 651j}{50 - 651j}$$

$$= 5 + \frac{775{,}000 - 10{,}090{,}500j}{426{,}301}$$

$$= 5 + \frac{775{,}000}{426{,}301} - \frac{10{,}090{,}500j}{426{,}301}$$

$$\boxed{Z_{L,18\text{W}} \approx 6.82 - 23.67j}$$

D. 20 W Oxygen Load

$$Z_L = 5 + \frac{1}{\frac{1}{275} + \frac{1}{-j1000} + \frac{1}{-j25}}$$

$$= 5 + \frac{1}{\frac{1}{275} + \frac{j}{1000} + \frac{j}{25}}$$

$$= 5 + \frac{1}{\frac{40}{11000} + j\frac{11}{11000} + j\frac{440}{11000}} = 5 + \frac{1}{\frac{40+451j}{11000}}$$

$$= 5 + \frac{11{,}000}{40 + 451j} \cdot \frac{40 - 451j}{40 - 451j}$$

$$= 5 + \frac{440{,}000 - 4{,}961{,}000j}{205{,}001}$$

$$\boxed{Z_{L,20\text{W}} \approx 7.15 - 24.20j}$$

We interpolated the load impedances for argon and oxygen by taking the average of the two measured operating-point impedances obtained. $Z_{\text{Ar,av}}$ and $Z_{\text{O,av}}$ serve as representative loads in the matching calculations.

$$\boxed{Z_{\text{Ar,av}} = \frac{1}{2}(7.05 - 22.54j + 5.8 - 22.7j) = 6.425 - 22.62j}$$

$$\boxed{Z_{\text{O,av}} = \frac{1}{2}(6.82 - 23.673j + 7.15 - 24.20j) = 6.985 - 23.9365j}$$

APPENDIX B
SMITH CHART WORK

In this section, we are going to show the Smith Chart work to obtain the stub length for the double stub matching network. In all cases, we found a set of stub length that does not lie in the forbidden zone.

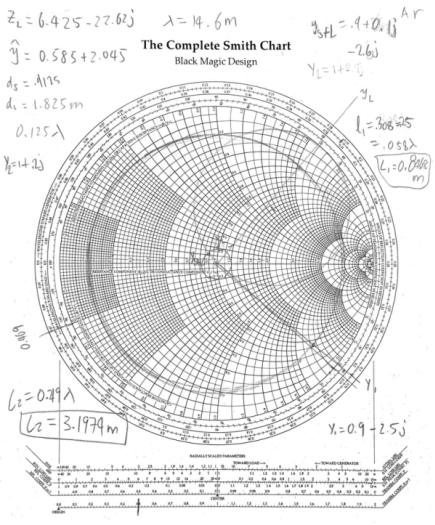

Fig. 8. Argon at 13.56 Mhz

Under 13.56 Mhz, Argron solutions are:

$$\boxed{L_1 = 0.8468 \text{ meters}; L_2 = 3.1974 \text{ meters}}$$

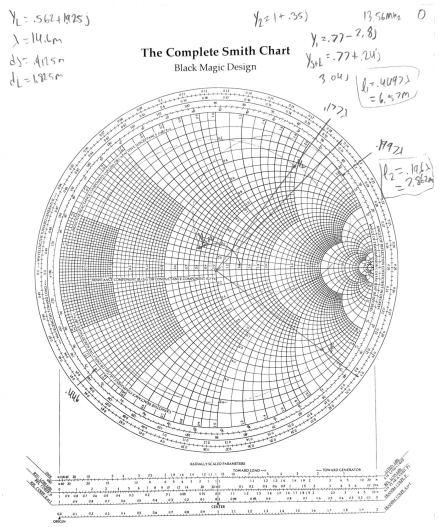

Fig. 9. Oxygen at 13.56 Mhz

Under 13.56 Mhz, Oxygen solutions are:

$$\boxed{L_1 = 6.57 \text{ meters}; L_2 = 2.862 \text{ meters}}$$

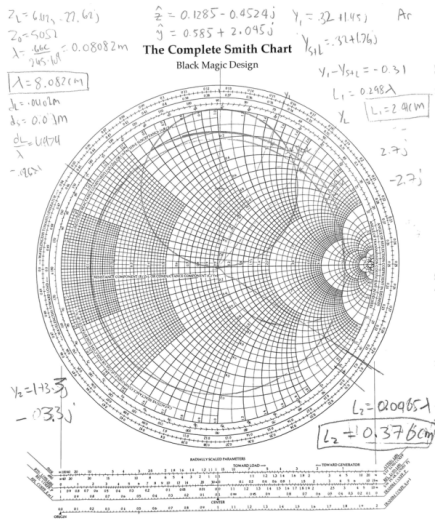

Fig. 10. Argon at 2.45 Ghz

Under 2.45 Ghz, Argon solutions are:

$$\boxed{L_1 = 0.0241 \text{ meters}; L_2 = 0.00376 \text{ meters}}$$

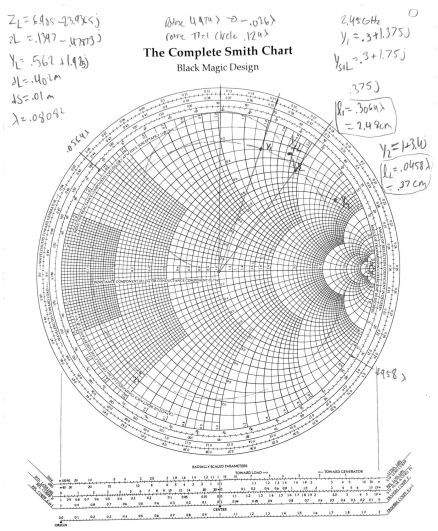

Fig. 11. Oxygen at 2.45 Ghz

Under 2.45 Ghz, Oxygen solutions are:

$$\boxed{L_1 = 0.0248 \text{ meters}; L_2 = 0.0037 \text{ meters}}$$

APPENDIX C
LC MATCHING SMITH CHARTS

Figure 12 illustrates the Smith chart construction used to design the LC matching network for the plasma load.

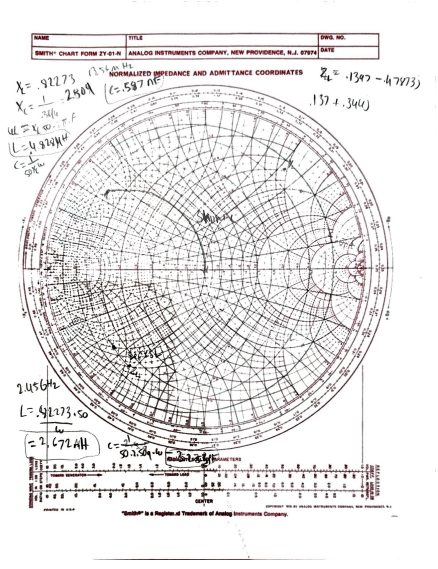

Fig. 12. Smith Chart Work for LC Matching.

APPENDIX D
LC MATCHING CALCULATION USING Q-FACTOR METHOD

In our work, the matched impedance is 50 Ω. For Argon, the predicted impedance in our model is

$$Z = 6.425 - j22.62 \ \Omega$$

Then, the Q-Factor Method work can be carried out

$$Q = \sqrt{\frac{50}{6.425} - 1} = 2.604$$

$$X_C = \frac{R_S}{Q} = \frac{50}{2.604} = 19.20 \ \Omega$$

$$X_L = Q \times R_{load} = 2.604 \times 6.425 = 16.73 \ \Omega$$

$$\boxed{X_{L_{total}} = X_L + X_R = 16.73 + 22.62 = 39.35 \ \Omega}$$

These are the values needed for calculation of capacitance and inductance. Specifically for 13.56 MHz:

$$\boxed{\begin{aligned} C &= \frac{1}{\omega X_C} = 611 \text{ pF}, \\ L &= \frac{X_L}{\omega} = 462 \text{ nH} \end{aligned}}$$

Similar process is done for 2.45 GHz:

$$\boxed{\begin{aligned} C &= \frac{1}{\omega X_C} = 3.384 \text{ pF}, \\ L &= \frac{X_L}{\omega} = 2.557 \text{ nH} \end{aligned}}$$

REFERENCES

[1] Diener electronic GmbH, "RF-Generator 13.56 MHz, 100 W," product datasheet, accessed Dec. 2025.
[2] Emblation Microwave, "ISYS245 Microwave System: Compact 100 W 2.45 GHz Microwave Generator and Amplifier," product brochure, accessed Dec. 2025.
[3] P. F. Ottinger, "Plasma Properties," Naval Research Laboratory, Washington, DC, USA, Technical Report NRL/PU/6790–05-491, 2005.
[4] P. S. Niklaus, M. M. Antivachis, D. Bortis, and J. W. Kolar, "Analysis of the Influence of Measurement Circuit Asymmetries on Three-Phase CM/DM Conducted EMI Separation," *IEEE Transactions on Power Electronics*, vol. 36, no. 4, pp. 4066–4080, 2021.
[5] Stephen Connell, "Procedure for designing a matching circuit using the Smith Chart," Lakes Region Repeater Association, Dec. 11, 2023. [Online]. Available: https://www.w1bst.org/procedure-for-designing-a-matching-circuit-using-the-smith-chart/.
[6] "47 CFR Part 18—Industrial, Scientific, and Medical Equipment," Electronic Code of Federal Regulations, Title 47, Subchapter A, Part 18, Federal Communications Commission, accessed Dec. 2025. [Online]. Available: https://www.ecfr.gov/current/title-47/chapter-I/subchapter-A/part-18.